Landscape and Urban Planning 222 (2022) 104395

Contents lists available at ScienceDirect

Landscape and Urban Planning

journal homepage: www.elsevier.com/locate/landurbplan

Research Paper

Viewshed-based modelling of visual exposure to urban greenery – An efficient GIS tool for practical planning applications

Zofie Cimburova[a,b,*], Stefan Blumentrath[a]

[a] Norwegian Institute for Nature Research (NINA), Sognsveien 68, NO-0855 Oslo, Norway

[b] Department of Architecture and Planning, Faculty of Architecture and Design, NTNU - Norwegian University of Science and Technology, NO-7491 Trondheim, Norway

HIGHLIGHTS

- We developed a geospatial method for modelling visual exposure to urban greenery.
- Implementing the method in GRASS GIS ensures its wide applicability and flexibility.
- High computational efficiency enables city-wide assessment on commodity hardware.
- Viewshed parametrisation and high-quality data needed for high modelling accuracy.

GRAPHICAL ABSTRACT

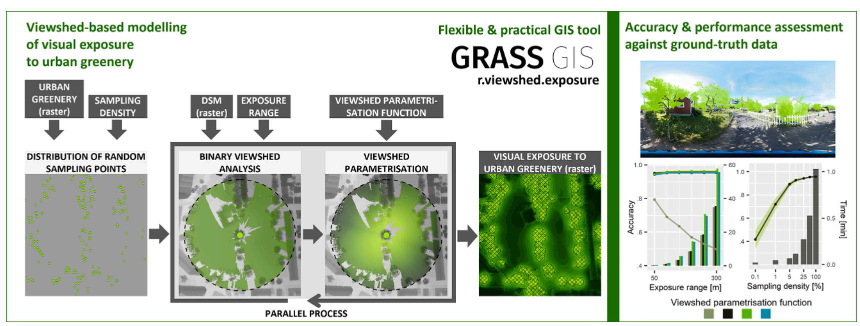

ARTICLE INFO

Keywords:
Urban greenery
Urban trees
Visual exposure
GIS
Viewshed analysis
Urban planning

ABSTRACT

Quantifying green visual exposure is necessary to assess aesthetic, social and health benefits from urban greenery. Viewshed analysis has been successfully used to model and map green visual exposure from human perspective in continuous representation and in places where street view imagery for widely-used photography-based methods is not available. However, current viewshed-based methods for modelling green visual exposure are often difficult to generalise beyond their specific application purpose, inefficient in processing large spatial extents and have limited use due to demands on technical knowledge. This hampers their wider use in research and practice. In this paper, we develop a viewshed analysis-based method for modelling visual exposure to urban greenery with special focus on the method's applicability in research and practice. The method is implemented as a tool in GRASS GIS which makes it available as a practical and flexible tool. Extensive validation and assessment of the method on the specific case of urban trees confirm that the method is a highly accurate alternative to modelling visual exposure from street view imagery ($\rho = 0.96$) but that data quality and viewshed parametrisation are essential for achieving accurate results. Thanks to parallel processing and effective implementation, the method is applicable for city-wide scale analysis with high-resolution data on commodity hardware (here illustrated on the case of Oslo, Norway). Therewith, the method has potential application in many areas including strategic tree planting, scenario modelling and urban ecosystem accounting, as well as ecosystem service research.

* Corresponding author.
E-mail address: zofie.cimburova@nina.no (Z. Cimburova).

https://doi.org/10.1016/j.landurbplan.2022.104395
Received 1 October 2021; Received in revised form 4 February 2022; Accepted 27 February 2022
Available online 4 March 2022

1. Introduction

Urban greenery has the potential to mitigate urban issues associated with rapid urban growth and climate change (Demuzere et al., 2014) by providing numerous ecosystem services (Millennium Ecosystem Assessment, 2003; TEEB, 2010), including temperature regulation, air and noise pollution mitigation, recreation opportunities and habitat for biodiversity (Bolund & Hunhammar, 1999; Gomez-Baggethun & Barton, 2013). This leads to economic, social, physical and mental health benefits and increases the wellbeing of urban citizens (Keniger et al., 2013; Office for National Statistics (ONS), 2019). An important pathway in receiving many benefits from urban greenery is visual exposure. Green visual exposure contributes to psychological, cognitive and physiological wellbeing (Kaplan, 2001; Lottrup et al., 2015; Ulrich, 1984). Further, visible greenery has aesthetic and amenity benefits (e.g., Schroeder & Cannon, 1983; Thayer & Atwood, 1978), thereby increasing neighbourhood walkability and property prices (Ki & Lee, 2021; Tyrväinen & Miettinen, 2000). Finally, green visual exposure leads to numerous social benefits, including reduced crime rates and increased perceived safety (e.g. Troy et al., 2012; Wolfe & Mennis, 2012; Mouratidis, 2019). Central to better understanding the relations between green visual exposure and associated benefits and applying these findings in practice is the possibility to quantitatively assess green visual exposure.

1.1. State of the art in quantitative assessment of green visual exposure

The amount of green visual exposure has traditionally been assessed manually. For instance, to study how street greenery affects health, De Vries et al. (2013) quantified visible greenery by direct observation in the field, while in the studies of Hazer et al. (2018) and Lottrup et al. (2015), the amount of visible greenery was self-reported by the study participants. Such manual approaches have been discussed as labour intensive and thus inefficient in large-scale field assessments and prone to human errors and bias due to observer subjectivity (Helbich et al., 2019). This hampers applying these approaches in e.g. dynamic green visual exposure assessment across space and time (Helbich, 2018) or urban planning applications.

In recent years, automatic methods for quantitative assessment of green visual exposure have been developed, focusing mainly on assessment from photographs and geospatial modelling. To our best knowledge, Aoki et al. (1985) were the first to measure the proportion of vegetation pixels in street photographs obtained from a human perspective and finding that it is an efficient measure of how much urban greenery people observe from a fixed observation point. The method has later been referred to as a Green View index (Yang et al., 2009) and gained attention and has been technically further developed thanks to the increased availability of street view images from databases of Google, Tencent or Baidu that minimise the need for manual photography (Helbich et al., 2019; Larkin & Hystad, 2019; W. Wang et al., 2019). However, the dependency on street images hinders applying the method in places and regions where street view imagery is not yet available (Rzotkiewicz et al., 2018) or where it usually is not obtained, such as backyards (Villeneuve et al., 2018). Because the green view index values are only available at photography points, the method is not suitable for purposes where continuous representation of green visual exposure is desired. Moreover, although the type of greenery affects the benefits obtained (Reid et al., 2017), photography-based methods usually do not enable such differentiation (Sun et al., 2021).

An alternative method that addresses many shortcomings of the photography-based methods is geospatial modelling of green visual exposure. It is not dependent on the availability of street view imagery and scales easily to large spatial extents. Raster-based geospatial analyses enable continuous representation of green visual exposure and can be used to analyse various types of urban greenery e.g., available from landcover maps provided by remote sensing (Yan et al., 2018). Numerous studies modelled green visual exposure with geospatial analysis as green coverage within properties, within specific radii from residence place or within census tracts (e.g., Troy et al., 2012; Ward Thompson et al., 2016; Wolfe & Mennis, 2012). Unlike photography-based methods, such aerial-perspective approaches however often fail to capture the amount of urban greenery visible from the perspective of people at ground level. The correlation between the amount of urban greenery observed from human versus aerial perspective is likely low (Helbich et al., 2019; Larkin & Hystad, 2019) or insignificant (R. Wang et al., 2019), and these two measures might capture different aspects of urban greenness (Falfán et al., 2018; Villeneuve et al., 2018).

A potentially powerful tool to reflect human visual perspective in geospatial modelling is viewshed analysis, which delineates the area visible from a given observation point, taking into account the surrounding terrain features (Petrasova et al., 2015). However, in green visual exposure modelling, viewshed analysis has been used sparsely (e.g., Łaszkiewicz & Sikorska, 2020; Nutsford, Pearson, Kingham, & Reitsma, 2016; W. Wang et al., 2019), and the potential for modelling green visual exposure in continuous representation remained largely unused, likely due to high computational workloads and dependency on high-resolution spatial data (Qiang et al., 2019; Tabrizian et al., 2020). Only recently have first studies begun experimenting with viewshed analysis to model green visual exposure in continuous representations and large-scale study areas. For example, Tabrizian et al. (2020) analysed the visibility of various vegetation classes from 39,321 viewpoints regularly displaced in a grid, and Labib et al. (2021) used viewshed analysis to assess visibility of greenery at all 86 million pixels of a region-wide raster map. The latter approach has recently been made available as an R-package (Brinkmann & Labib, 2021). These studies showed that geospatial modelling with viewshed analysis can successfully be used to model green visual exposure from human perspective, in continuous representation, in large spatial extents and at places where street view imagery is unavailable.

However, several challenges hinder wider applicability of these novel methods. First, the method settings (e.g., exposure range) have often been fixed for specific application purposes, which hampers their generalisation outside the original scope. In addition, the sensitivity of modelling accuracy to those settings has not been systematically studied (Labib et al., 2021), and current methods do not offer the flexibility to conduct such assessment. Second, the methods are often provided as scripts, and their usage requires a higher degree of technical knowledge, which limits their practical applicability. Third, analysing large spatial extents, such as entire cities, in large detail can take significant amount of time, even when using high-performance computing systems which are not commonly available to practitioners and require significant technical skills (Labib et al., 2021).

1.2. Paper objectives

Our aim in this paper is to build on the work of Labib et al. (2021) and Tabrizian et al. (2020) and develop a viewshed-based method for modelling visual exposure to urban greenery with special focus on the method's general applicability in research and practice. In particular, the method should be (i) integrated as a tool in open-source geographical information system (GIS) to lower the threshold for usage and to increase the method's flexibility, thus enabling adjusting the method to different application purposes and simplifying empirical assessment of the method's settings in relation its performance, (ii) empirically assessed against ground-truth to demonstrate how the settings influence the method's performance in terms of accuracy and processing time, which also provides guidelines for application of the method in praxis and (iii) computationally efficient so that large spatial extents and high-resolution datasets can be analysed on commodity hardware.

The method is assessed on the specific case of urban trees but can be applied similarly to analyse visual exposure to other types of urban greenery. Urban trees are used for three reasons. First, trees are an urban asset often managed and valued separately from other greenery (Nowak, 2017). Second, the benefits obtained by visual exposure to trees might be different from those of other types of urban greenery (Reid et al., 2017). Finally, trees significantly impact green visual exposure due to their vertical dimension and are thus an effective way of creating green views in urban areas where space is often limited (Yang et al., 2009).

2. Methods

2.1. Background of visibility modelling in geospatial analysis

The method for modelling visual exposure to urban greenery is based on viewshed analysis, a geospatial analysis method applied to a digital surface or terrain model that delineates the area (viewshed) visible from a given pixel (observation point) by determining whether the view between the observation point and all other pixels (target points) within a given radius is obstructed. The analysis returns a map where visible and non-visible pixels are usually coded as 1 and 0, respectively (Petrasova et al., 2015).

Research suggests that a binary viewshed representation – with visible and non-visible pixels – does not accurately reflect visibility from human perspective because it fails to account for the variable visual significance of the observable objects from the observer's point of view (Chamberlain and Meitner, 2013; Ervin and Steinitz, 2003; Nutsford et al., 2015; Ogburn, 2006). The visual significance is affected by the properties of the observed objects (e.g. size, contrast between the object and surroundings), observer's characteristics (e.g. visual acuity and resolving capacity of human eye), the environment between the observed objects and the observer (e.g. light and atmospheric conditions) and their relative spatial configuration (e.g. distance, slope and aspect) (Domingo-Santos, 2017; Groß, 1991; Ogburn, 2006).

Therefore, various viewshed parametrisation functions have been developed, where focus was put mainly on accounting for the effect of spatial configuration between the observed objects and the observer (e.g. Chamberlain and Meitner, 2013; Domingo-Santos et al., 2011; Grêt-Regamey et al., 2007; Nutsford et al., 2015). These functions build on the concepts of solid angle (Groß, 1991), visual magnitude (Iverson, 1985; Travis et al., 1975) and vertical visual angles (Llobera, 2003). Visual magnitude and vertical visual angle quantify the portion of the observer's field of view occupied by the observed object, depending on its slope, aspect and distance relative to the observer. Solid angle is a direct measure (in steradians) of the surface area of the observer's eye retina covered by the projection of the observed object. Another approach is fuzzy viewshed analysis which simulates the decreasing clarity of the observed objects with increasing distance from the observer due to atmospheric and lighting conditions (Fisher, 1994; Ogburn, 2006).

In this paper, we implement the visual magnitude algorithm of Chamberlain and Meitner (2013) and the solid angle algorithm of Domingo-Santos et al. (2011). We further implement a simple exponential distance decay function used in the visual magnitude algorithms of Chamberlain and Meitner (2013) and Grêt-Regamey et al. (2007) to see whether the sole effect of distance (i.e. omitting slope and aspect) can adequately capture the visual impact of greenery. We do not implement the fuzzy viewshed function because atmospheric extinction is likely a minor issue for green visual exposure in urban areas. The individual viewshed parametrisation functions are described in the Supplementary Material.

Of specific relevance for modelling visual exposure is analysing the composition of the viewshed, i.e. the portion of viewshed made up by the studied exposure source, here urban greenery. This analysis, also referred to as viewscape analysis (Tabrizian et al., 2020), has been used previously in landscape aesthetics assessment (Grêt-Regamey et al., 2007), hedonic pricing studies (Bishop et al., 2004) or to study how view characteristics affect mental health (Nutsford et al., 2016; Tabrizian et al., 2020). To achieve an area-wide, continuous representation of visual exposure, the analysis of viewshed composition is usually calculated for all possible observation points (pixels) that make up the study area (Labib et al., 2021; Tabrizian et al., 2020). However, such a procedure is computationally intensive, especially if the spatial extent or resolution of the analysed area is large. If the number of possible observation points is larger than the number of pixels representing the exposure source, the computational efficiency can be increased by reversing the perspective and taking the observation points as targets and the exposure source pixels as observers, assuming their mutual visibility. Viewsheds calculated from the exposure source pixels represent the areas visually exposed to that pixel. Such an approach is often used in visual impact assessment (e.g. Minelli et al., 2014; Ogburn, 2006). Adding up the individual viewsheds then results in a continuous representation of visual exposure, referred to as a cumulative viewshed (Wheatley, 1995). Such modelling approach also seems suitable for the method developed in this paper, as in urban areas, the number of possible observation points is often larger than the number of green pixels. In addition, we hypothesise that computing visual exposure from a random sample of all exposure source pixels can yield adequate accuracy while decreasing processing times significantly, especially when analysing large-extent, high-resolution datasets.

2.2. Method development

2.2.1. Processing workflow

Input spatial datasets to the developed method are (i) a raster map of urban greenery and (ii) a high-resolution digital surface model (DSM). A DSM is a continuous representation of surface heights, including built and natural structures such as trees. Importantly, a DSM is a 2.5D representation of space, i.e. all surface locations have single elevation information. The processing workflow of the method consists of four steps (Fig. 1). First, the input map of urban greenery is randomly sampled by vector points in specified sampling density. The second and third step are executed iteratively for each sampling point. In the second step, a binary viewshed is generated from the sampling point. The point height above the DSM is 0 m (i.e. the viewshed is generated from surface of the greenery). The user can control the height of the observer on the ground and viewshed radius (i.e. range of visual exposure). In the third step, the binary viewshed can be parametrised by one of the three implemented viewshed parametrisation functions (solid angle, visual magnitude, distance decay). Finally, visual exposure values from viewsheds generated from all sampling points are added, resulting in a continuous raster map of visual exposure to urban greenery.

2.2.2. Method implementation

The method was implemented as a tool ("AddOn") called *r.viewshed.exposure* to the Geographic Resources Analysis Support System (GRASS) GIS, which is a cross-platform multi-purpose GIS software offering more than 300 analytical tools and a growing number of AddOns that extend the core functionality. The source code of GRASS GIS is available under the GNU General Public License (Neteler et al., 2012). GRASS GIS offers the underlying functionality that makes it a suitable platform for implementing the method developed in this paper, namely an efficient tool for viewshed analysis *r.viewshed* (Toma et al., 2020) and a comprehensive Python API, including integration with NumPy.

We wrote the algorithm of *r.viewshed.exposure* with computational efficiency in mind. For example, many operations of the algorithm are conducted in memory, reducing the time needed for writing and reading operations. Computational efficiency was further increased by parallelizing the iterative operations. To enable wide usage of *r.viewshed.exposure* in practical applications, sampling density, observer height, visual exposure range and viewshed parametrisation function were implemented as user-specified settings.

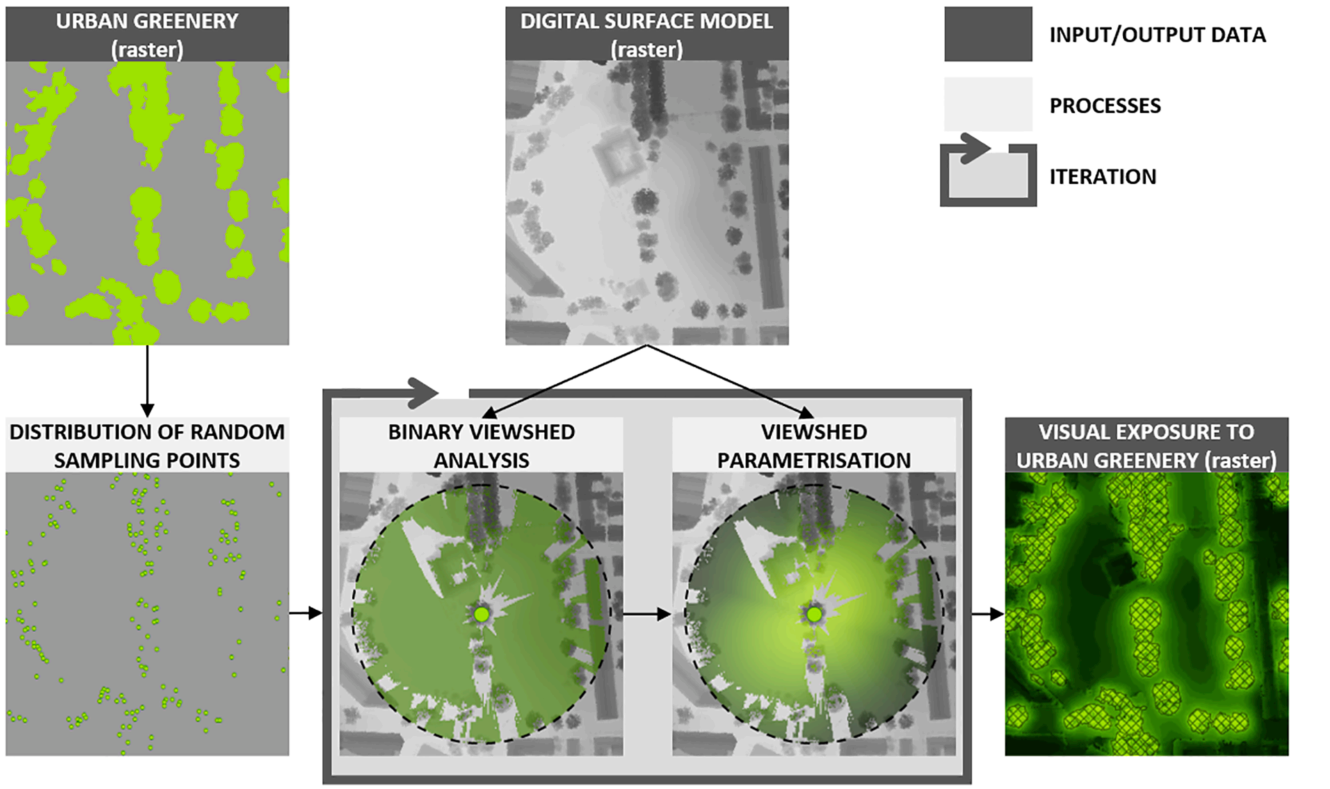

Fig. 1. Processing workflow of the developed method for modelling green visual exposure. (For interpretation of the references to colour in this figure legend, the reader is referred to the web version of this article.)

2.3. *Method assessment*

The method was assessed on the specific case of urban trees from two perspectives. First, we assessed the method against ground-truth data to see how the method's accuracy and processing time vary in response to the method's settings. Second, we assessed the computational efficiency of the method in a city-wide application with high-resolution data.

2.3.1. *The effect of variation in the method's settings*

The method was assessed by comparing values of visual exposure to urban trees modelled with *r.viewshed.exposure* against percentage of tree canopy manually delineated in full view (360° × 180°) panoramas obtained at 94 validation points, randomly distributed in sampling areas stratified across 11 urban form types of Oslo, Norway. Measuring the percentage of greenery in photographs is a common method to assess the amount of greenery observed from a human perspective (Yang et al., 2009). Each validation point was associated with accurate geographic coordinates to extract the modelled values of visual exposure and obtain the validation photographs at the same location. A detailed description of the process of obtaining validation data is provided in the Supplementary Material.

The settings of *r.viewshed.exposure* (viewshed parametrisation function, exposure range, sampling density, input data quality) were systematically tested in three steps (Table 1). In the first step, accuracy and processing time were recorded for all possible combinations of viewshed parametrisation functions and exposure ranges between 50 m and 300 m with 50 m steps. This was done to determine the method's highest possible accuracy and see how these settings affect the trade-off between accuracy and processing time. Exposure ranges larger than 300 m were not tested due to increased processing time and observable saturation with regards to accuracy. Sampling density was 100%. The input exposure source map was a tree canopy dataset in 1 m resolution obtained by laser scanning in 2017 (Hanssen et al., 2021). This is the most precise spatial representation of tree canopy currently available for the built-up area of Oslo. However, due to low accuracy at individual tree level, we manually corrected the dataset around the validation points using an updated orthophoto.

In the second step, we varied sampling density between 0.1%, 1%, 5%, 10%, 25%, 50% and 100% and observed its effect on the accuracy/processing time trade-off. We used the combination of viewshed parametrisation function and exposure range identified in the first step as a good trade-off between accuracy and processing time. For sampling densities lower than 100%, the modelling was repeated 50 times to account for randomness in sampling point distribution and provide a more robust accuracy estimate. The average accuracy and standard deviation across the 50 repeats were reported.

Table 1
Settings of r.viewshed.exposure used in method assessment.

	Viewshed parametrisation	Exposure range	Sampling density	Tree canopy map resolution	DSM resolution
Step 1: Test of viewshed parametrisation & exposure range	None; Distance decay; Visual magnitude; Solid angle	50 m; 100 m; 150 m; 200 m; 250 m; 300 m	100%	1 m	1 m
Step 2: Test of sampling density	Determined by step 1	Determined by step 1	0.1%; 1%; 5%; 10%; 25%; 50%; 100%	1 m	1 m
Step 3: Test of input data quality	Determined by step 1	Determined by step 1	100%	10 m	1 m

Finally, in the third step, we run *r.viewshed.exposure* with a 10 m tree canopy map derived from Sentinel-1 and Sentinel-2 imagery (Venter and Sydenham, 2021) to assess how input data resolution affects accuracy. Sampling density was set to 100%, and except for the tree canopy map, the same settings as in the previous steps were used.

In all three steps, the input surface model was a 1 m DSM obtained by laser scanning (Norwegian mapping authority, 2019) and exposure receiver height was 150 cm, consistently with the shooting height of validation panoramas. *r.viewshed.exposure* was run on 25 cores of an HPE ProLiant DL360 Gen10 server with two Intel(R) Xeon(R) Gold 6134 CPU @ 3.20 GHz Central Processing Units, 256 GB Random Access Memory and three 960 GB Solid State Storage Devices with 6Gbps bandwidth and ext4 file system running Ubuntu 18.04.5 LTS. Accuracy was assessed by Spearman correlation coefficient (ρ) between the percentage of tree canopy pixels in the validation panoramas and values extracted from the maps modelled with *r.viewshed.exposure*. Processing time was measured as a per-point elapsed time, i.e. the average elapsed time of running *r.viewshed.exposure* within the specified exposure range of one validation point, where the grid size to process in number of pixels is the square of exposure range.

2.3.2. City-wide application

To assess the method's computational efficiency in a practical city-wide application with high-resolution data, we ran *r.viewshed.exposure* for the entire study area of Oslo. We used the same input data (1 m tree canopy map and DSM) and server as in the first assessment phase. The total extent of the study area was 19603 × 18486 pixels, covering 152 km^2, i.e. 152 million non-null pixels, out of which 49.5 million pixels was tree canopy. For viewshed parametrisation function, exposure range and sampling density, we used the combination identified as a good trade-off between accuracy and processing time in the first assessment phase.

3. Results

3.1. *r.viewshed.exposure*

The developed tool *r.viewshed.exposure* (Fig. 2) is available through the GRASS GIS Addons repository. The default values of viewshed parametrisation function, exposure range and sampling density are set to the combination identified as a good trade-off between accuracy and processing time in the method assessment. Fig. 3 provides examples of maps of visual exposure to urban trees calculated with the tool using the different viewshed parametrisation options, 200 m exposure range and 100% sampling density. While all three viewshed parametrisation functions lead to visually similar output, the map created without viewshed parametrisation is significantly different. The range of numerical values of visual exposure depends on viewshed parametrisation, exposure range, sampling density and spatial resolution of the analysis. We include detailed information about theoretical value ranges of the individual functions in the Supplementary Material.

3.2. Method assessment

3.2.1. The effect of variation in the method's settings

The highest Spearman correlation coefficient between values of visual exposure to urban trees modelled with *r.viewshed.exposure* and the percentage of tree canopy in validation panoramas is 0.96 (solid angle function, 200 m exposure range, 100% sampling density). This means that the developed method captures visual exposure to urban trees almost as accurately as street view photographs. In Fig. 4, the modelled values are plotted against the tree canopy percentage. At visual inspection, the relationship is clearly monotonic. The scatter plot also identifies cases where the modelled values considerably under- and over-estimate the tree canopy percentage (points O1 and O2). In these outlying validation points, tree canopy percentage was measured in photographs taken from under the tree canopy, while visual exposure was modelled on the surface of the tree canopy due to the 2.5D character

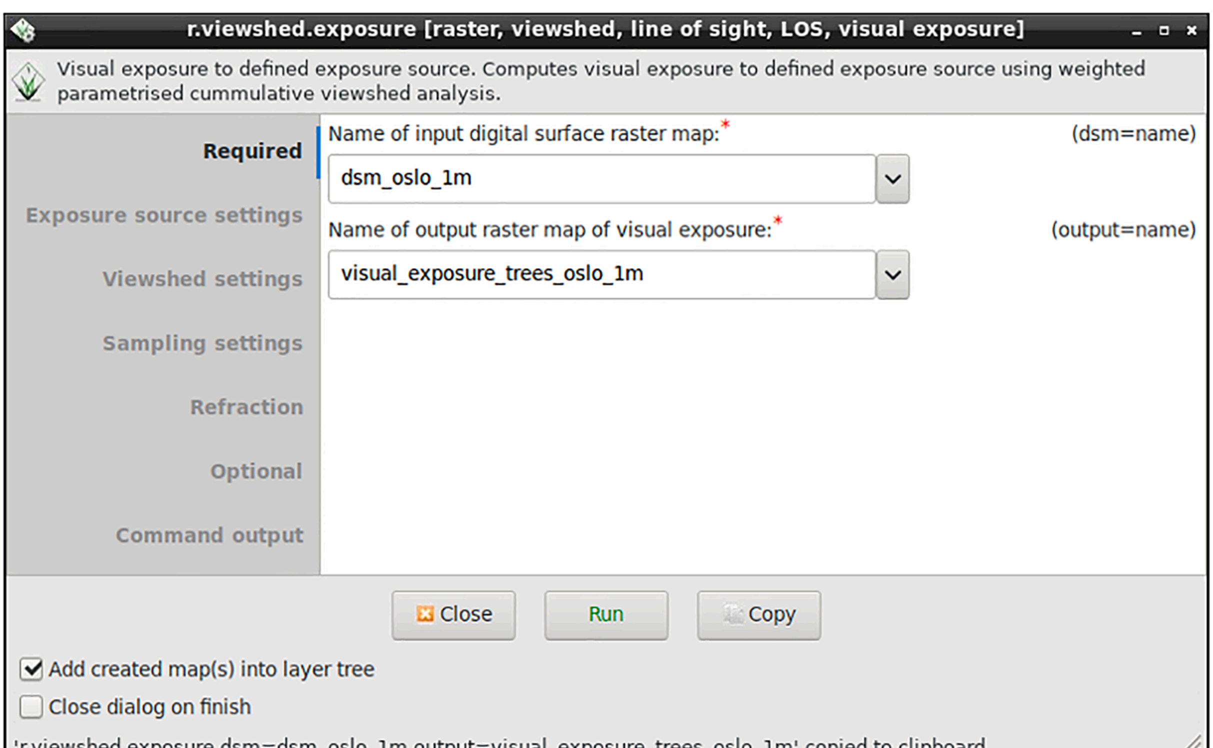

Fig. 2. Graphical user interface of *r.viewshed.exposure* in GRASS GIS.

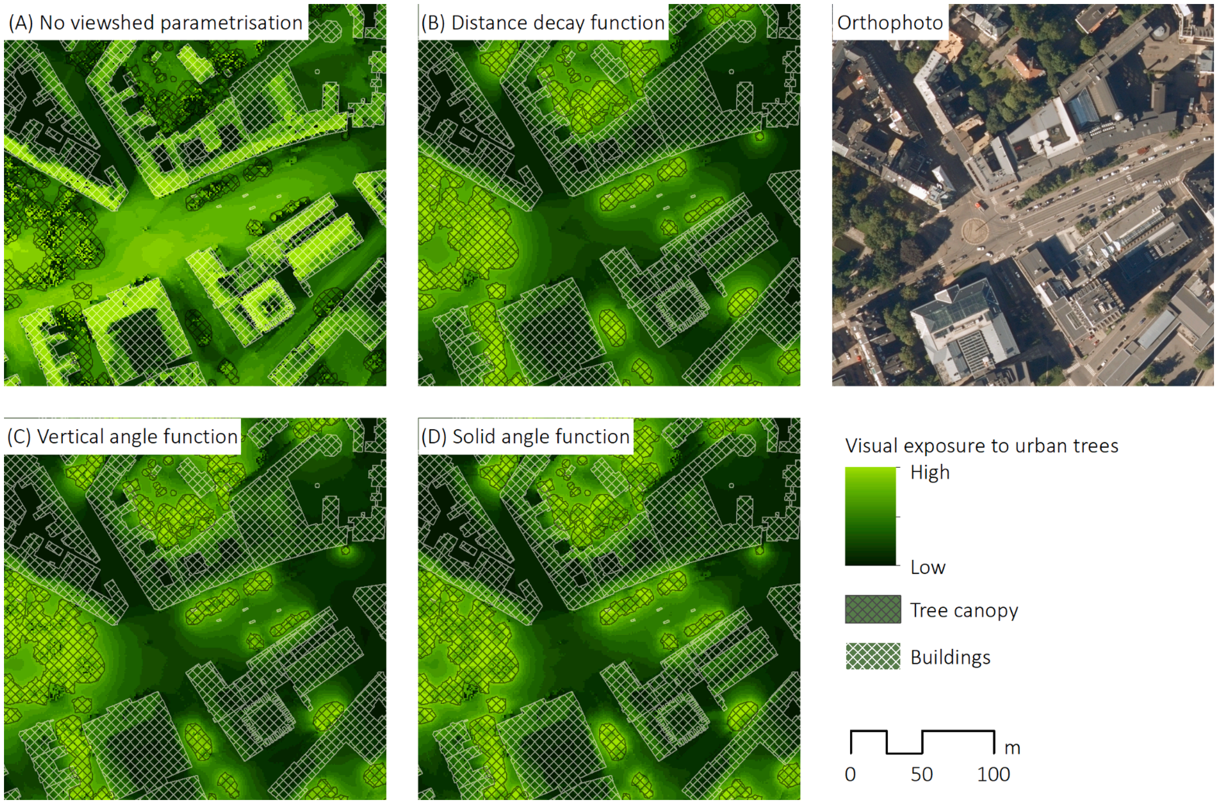

Fig. 3. Visual exposure to urban trees modelled with *r.viewshed.exposure* (200 m exposure range, 100% sampling density). (For interpretation of the references to colour in this figure legend, the reader is referred to the web version of this article.)

of the DSM. Fig. 4 further illustrates the range of modelled visual exposure values across the validation points, along with output maps and validation panoramas.

Fig. 5A illustrates that the accuracy differs little between viewshed parametrisation functions (ρ = 0.94–0.96) while omitting viewshed parametrisation leads to significantly lower accuracy (ρ = 0.50–0.79). This underpins the importance of viewshed parametrisation when modelling visual exposure to urban trees. Solid angle and visual magnitude functions increase processing time roughly 1.6x compared to no parametrisation and distance decay function (Fig. 5A). Considering that both former functions do not significantly improve accuracy, the simpler distance decay function can be a good choice for many applications.

Fig. 5A further shows that exposure range has minimal effect on accuracy if viewsheds are parametrised (ρ = 0.94–0.96), although 50 m exposure range has slightly lower accuracy in all three parametrisation functions. Yet, without viewshed parametrisation, accuracy clearly decreases with increasing exposure range. This is likely caused by the disproportional increase in visual exposure due to increasing number of visible pixels at longer exposure ranges. The relationship between exposure range and per-point elapsed time follows a power function across all viewshed parametrisation options. Therefore, lower exposure ranges can be a good choice for reliable and efficient modelling of visual exposure to urban trees from human perspective. Considering the abovementioned findings, we used distance decay function and 100 m exposure range to assess the effect of sampling density and input data accuracy.

Fig. 5B shows that low sampling density (0.1%, 1%) leads to low accuracy with high uncertainty due to the randomness in sampling point distribution (ρ = 0.42 + -0.079 and 0.72 + -0.051, respectively). However, with sampling density 25% and higher, accuracy is comparable to 100% sampling density and the uncertainty is low (ρ = 0.94 + -0.009). Processing time increases exponentially with increasing sampling density and e.g. with 25% sampling density, the processing time is nearly four times shorter compared to 100% sampling density.

Using a low-resolution tree canopy map, the accuracy dropped considerably (ρ = 0.53). This indicates that input data quality impacts the result accuracy even more than viewshed parametrisation and exposure range (except for extreme settings without viewshed parametrisation).

3.2.2. *Visual exposure to urban trees in Oslo*

The result of running *r.viewshed.exposure* for the extent of Oslo with distance decay parametrisation function, 100 m exposure range and 25% sampling density is illustrated in Fig. 6 and also provided as an interactive map at http://urban.nina.no/maps/400/view. The total elapsed time was 133.8 h.

4. Discussion

In this paper, we built upon the work by Labib et al. (2021) and Tabrizian et al. (2020) and developed a viewshed-based method for modelling visual exposure to urban greenery. The method supports the potential of geospatial modelling to address shortcomings of photography-based methods for quantifying visual exposure to urban greenery (Helbich et al., 2019; Larkin & Hystad, 2019; W. Wang et al., 2019; Yang, Zhao, McBride, & Gong, 2009). In particular, the method developed here can model visual exposure to various types of urban greenery (here illustrated on the case of urban trees), which usually is not possible with photography-based methods (Sun et al., 2021). In addition, the method enables modelling green visual exposure in continuous representation and in places and regions where street view imagery is not available (Rzotkiewicz et al., 2018; Villeneuve et al., 2018).

The method has been developed with particular focus on its usability in research and practical applications. It was implemented as a GIS tool

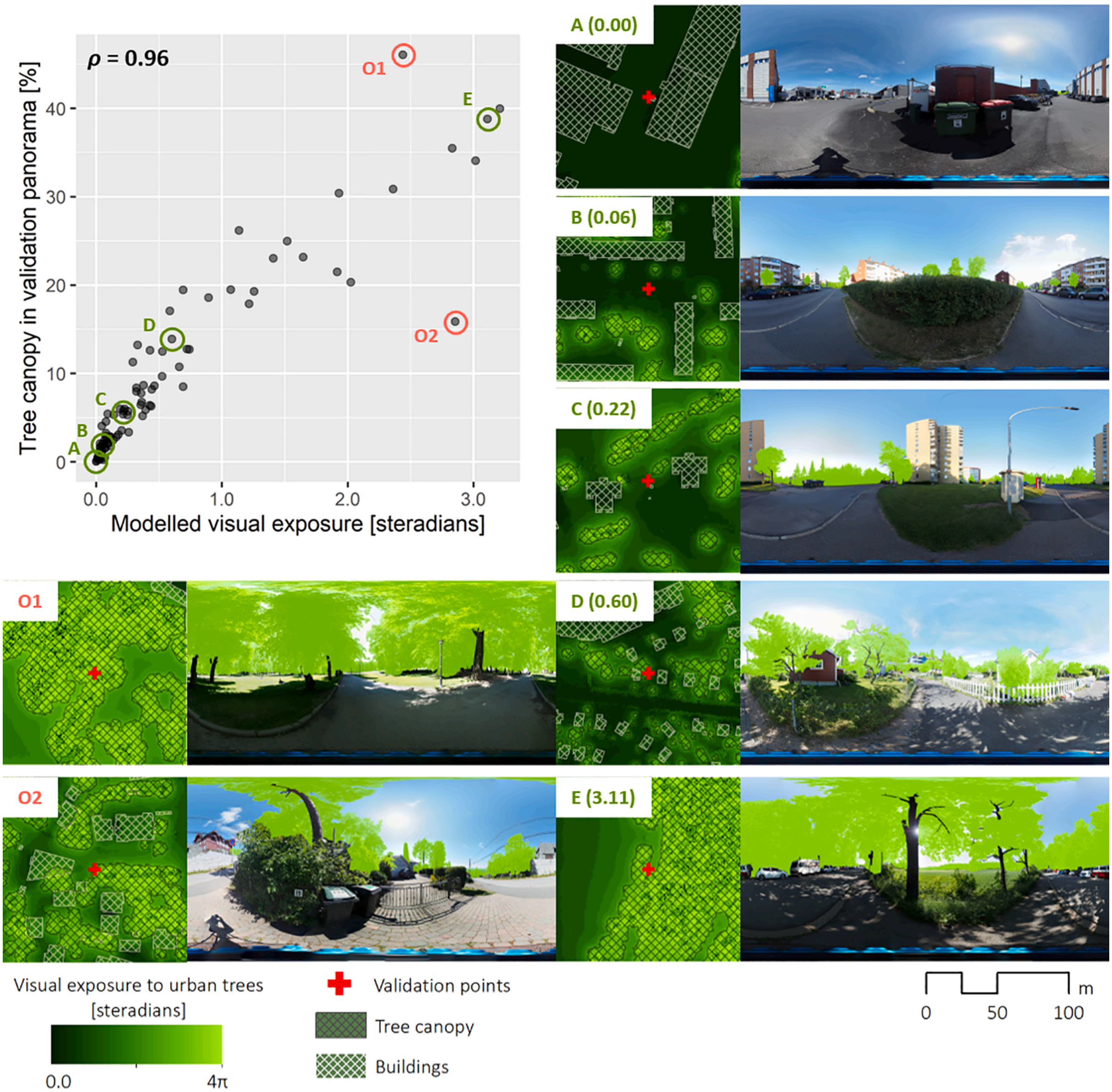

Fig. 4. Values of visual exposure to urban trees modelled with *r.viewshed.exposure* at validation points (solid angle function, 200 m exposure range), plotted against tree canopy percentage, and value range of modelling results. (For interpretation of the references to colour in this figure legend, the reader is referred to the web version of this article.)

to lower the threshold for usage and with several user-specified settings to increase its flexibility, which is especially valuable for research. At the same time, the method was extensively assessed on the case of urban trees, which makes its applicability in practice easier. Furthermore, the general usability of the method is ensured by its high computational efficiency. In the following, we discuss this in more detail.

4.1. Method implementation in GRASS GIS

The method was implemented as a tool called *r.viewshed.exposure* in GRASS GIS. This lowers the technical demands on the users and enables direct integration of the method in the users' GIS workflows. Furthermore, user-specified settings like viewshed parametrisation function, exposure range, sampling density and observer height increase the method's flexibility and thereby enable adjusting it to specific needs of various application purposes. This flexibility also facilitates systematic validation and assessment of the method in various contexts and thus contributes to building knowledge about the visual effects of urban greenery. The integration of the method in open-source GIS ensures that the method can be improved beyond the current state, for instance by implementing new viewshed parametrisation functions.

4.2. Method assessment

The method was empirically assessed to see how its settings influence the performance in terms of accuracy and processing time. The findings provide important insight for application purposes where a minor accuracy loss might be acceptable in return for shorter processing time – for instance for planning purposes on city scale, where the processing extent is often large but computational resources may be limited. Furthermore, the findings about individual settings provide information about the "default values" to use in practical applications.

The assessment showed that the values of visual exposure to urban trees modelled with the developed method are highly correlated to tree canopy percentage in street view panoramas. Thus, the developed method is a reliable alternative for quantifying visual exposure to urban

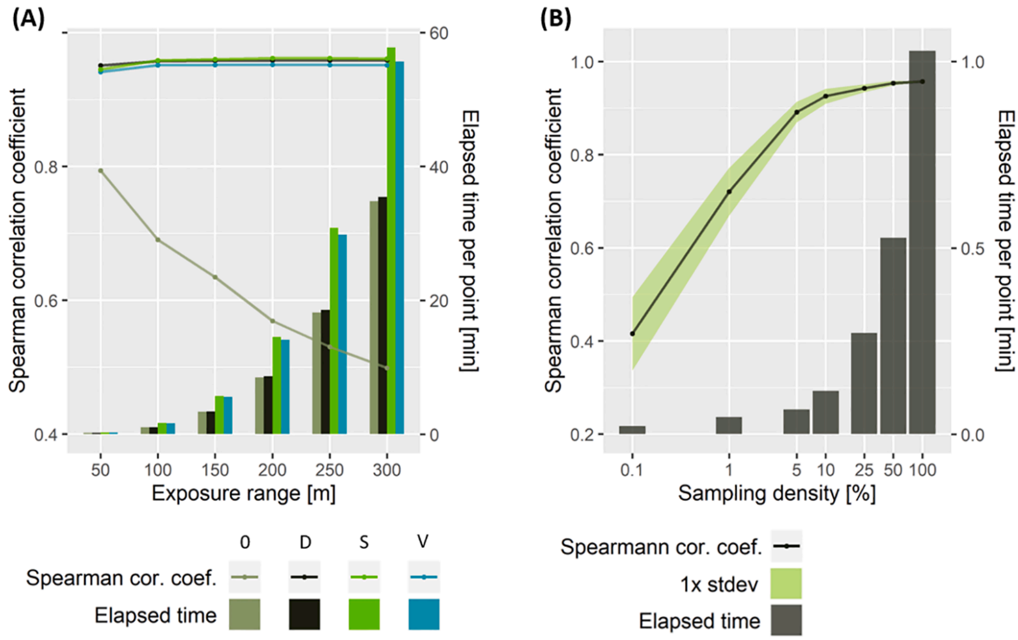

Fig. 5. (A) Effect of exposure range and viewshed parametrisation on method performance (100% sampling density). 0, D, S and V refer to no parametrisation, distance decay function, solid angle function and visual magnitude function, respectively. (B) Effect of sampling density on method performance (distance decay function, 100 m exposure range). X-axis is logarithmically scaled. (For interpretation of the references to colour in this figure legend, the reader is referred to the web version of this article.)

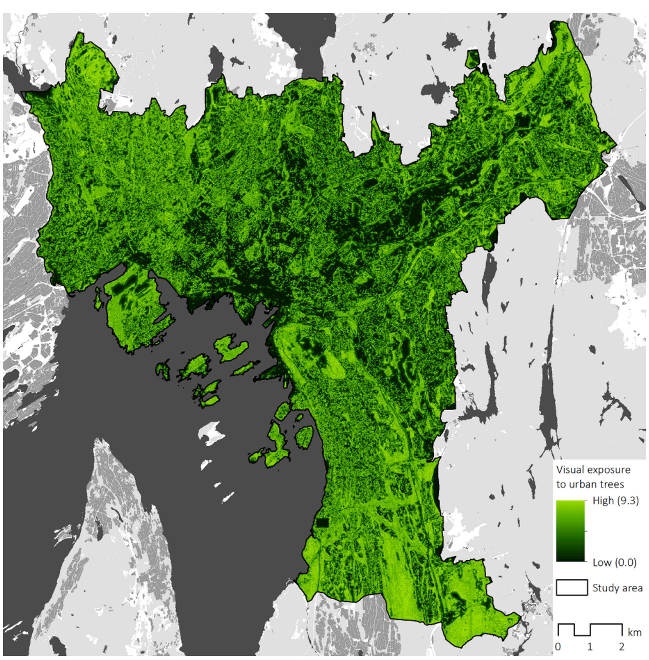

Fig. 6. Visual exposure to urban trees in Oslo (distance decay function, 100 m exposure range, 25% sampling density). (For interpretation of the references to colour in this figure legend, the reader is referred to the web version of this article.)

trees. With a Spearman correlation coefficient of up to 0.96, the degree of correlation is significantly higher than the correlation reported for the method by Labib et al. (2021) (Pearson correlation coefficient 0.481). Apart from potential differences in viewshed computation and different correlation measures used, the lower correlation in Labib et al. (2021) may be attributed to different studied greenery types (all greenery vs only trees), lower input data resolution and different viewshed parametrisation function. The assessment further confirmed that the method is not suitable for modelling visual exposure under tree canopies. This is due to the 2.5D character of the DSM, where all surface locations have single elevation information. In turn, visual exposure values at tree locations represent the amount of tree canopy visible from the surface of the trees, not from under them. For the same technical reason, the method cannot model green visual exposure from vertical surfaces (e.g., from building facades to assess the exposure of building occupants). In further development, the method could therefore be adjusted to operate with 3D models (Bishop, 2003) or to minimise the effect of trees on view obstruction (Murgoitio et al., 2013).

In line with previous studies (Domingo-Santos, 2017; Groß, 1991; Ogburn, 2006), the assessment further underpinned the importance of parametrising the binary viewshed to better reflect visual significance of observed objects. All three parametrisation functions implemented in *r.viewshed.exposure* significantly improved the method's accuracy. Compared to the distance decay parametrisation function used in Labib et al. (2021), the functions in *r.viewshed.exposure* have significantly steeper slope. Given the high accuracy, we hypothesise that such steeper functions are more suitable for modelling visual exposure in urban areas. Further, we hypothesise that visual exposure to urban trees is mainly influenced by the distance between the observer and the observed object because including their relative slope and aspect did not significantly increase the accuracy. Larger exposure ranges did not increase accuracy but considerably increased processing time. Therefore, relatively short exposure ranges (100 m) might be sufficient for accurate and fast green visual exposure modelling in urban settings, where surrounding structures often limit visibility at relatively low distances. This is in accordance with studies of Łaszkiewicz and Sikorska (2020), R. Wang et al. (2019) and W. Wang et al. (2019). On the other hand, longer ranges are often used in regional or landscape scales (Brabyn, 2015; Fisher, 1994). In general, further research is needed to systematically check how the shape of viewshed parametrisation functions and exposure ranges affect the results.

Finally, the assessment underpinned the need for using high-resolution high-quality input spatial data because these influence the underlying viewshed analysis (Ervin and Steinitz, 2003). The visibility of greenery in urban areas is often affected by relatively small details in the physical urban structure, which are only represented in high-resolution surface models (e.g., individual trees, walls). The availability of high-quality input data might limit the application of the method, however, access to such data from laser scanning or Unmanned Aerial Vehicles increases due to technical development.

Photography-based methods to quantify green visual exposure (Helbich et al., 2019; W. Wang et al., 2019; Yang et al., 2009), here used to validate and assess the developed method, are based on the assumption that the amount of greenery measured from photographs reflects the amount of greenery observed by people. However, researchers disagree on the extent to which photographs really capture what people see (compare e.g., Aoki et al. (1985) and Falfán et al. (2018)), for instance due to observer characteristics (Falfán et al., 2018) or photograph distortion due to lens settings and panorama projections (Aoki et al., 1985; Zelnik-Manor et al., 2005). The values of visual exposure to urban greenery measured from photographs or modelled by *r.viewshed.exposure*, therefore, represent a measure of potentially visible greenery from human perspective (Falfán et al., 2018). An important next step would be to assess the correspondence between these objective modelled/measured values and subjective, self-reported perceived green visual exposure. Moreover, research suggests that quality of greenery also determines the benefits obtained (Reid et al., 2017). Therefore, the method could be further extended to enable weighting the individual viewsheds by quality of greenery, if such data are available for instance from remote sensing (Yan et al., 2018).

The findings regarding accuracy, viewshed parametrisation functions and exposure ranges are based on an assessment conducted across different urban form types in Oslo. However, the suitability of different combinations of the method's settings might vary with urban form types. For instance, while a short exposure range might provide sufficient accuracy in a dense urban centre, longer exposure ranges might perform better in low-density suburbs. This might be important information to consider in application purposes targeted at specific urban form type. Caution should also be paid when generalising the findings to study areas with significantly different urban morphology than Oslo. An important next step would therefore be to systematically assess the sensitivity of the method's setting to different urban form types and explore the method's performance in other study areas.

Similarly, caution needs to be paid when generalising the findings to other types of greenery than urban trees. Urban trees have a specific visual impact due to their vertical dimension, while other types of urban greenery (e.g. grass, low shrubs) are mostly horizontal, and their visual impact might be different. Future studies could therefore assess the developed method on other types of urban greenery.

Future work should also focus on clarifying the range of numerical values of green visual exposure resulting from the modelling. The range can vary significantly, depending on viewshed parametrisation function, exposure range, sampling density and resolution of the underlying spatial data. This also hinders further interpretation of the numerical values. Previous studies expressed the modelled green visual exposure values as a proportion of total viewshed comprising urban greenery (Labib et al., 2021; Łaszkiewicz & Sikorska, 2020), which is easy to interpret, or as absolute values (Domingo-Santos et al., 2011; Nutsford et al., 2015), as in this study, where interpretation is more challenging.

4.3. Computational efficiency

The method can be efficiently run on a personal computer or server, which is especially beneficial in daily planning practice and small-scale studies. Its ability to efficiently process large spatial extents at fine detail is likewise advantageous in large-scale studies. Compared to the method of Labib et al. (2021), *r.viewshed.exposure* is significantly faster. Direct comparison to the performance of the method by Labib et al. (2021) is not possible due to different hardware and input data used. The city-wide applications however give some general hints. The amount of data processed for Oslo is roughly twice the amount in Labib et al. (2021) (152 and 86 million pixels, respectively), while processing time is less than half (5.6 and 11.5 days, respectively). As a rough estimate, assuming that the computer used in this study computes at the same speed as reported by Labib et al. (2021) (0.8 s per viewshed), processing time for their method applied to the Oslo dataset would have been ~1680 h (or 70 days). Several factors contribute to computational efficiency of *r.viewshed.exposure*. First, the processing workflow reduces the number of viewshed operations by only processing green pixels. Areas with little greenery are therefore processed faster than equally large areas with high green coverage. Second, the assessment showed that computational time can be significantly reduced by decreasing exposure range and sampling density of the input map, with limited effect on the accuracy. Finally, the method is implemented using effective in-memory operations and process parallelisation. For very large rasters, memory consumption might become a bottleneck, but this can be addressed by processing data in chunks (tiled processing). GRASS GIS offers off-the-shelf solutions for that if necessary.

4.4. Relevance for urban planning and research applications

The method developed in this paper is relevant for numerous urban planning and policy applications. First, urban foresters can use the green visual exposure map for awareness-raising amongst the public. Second, the method provides useful input into urban ecosystem accounting, as it enables documenting and reporting on the temporal changes of green visual exposure, for example following tree planting programs. The results of green visual exposure modelling can also be aggregated and used in comparisons of neighborhoods or cities. Third, in strategic tree planting, the visual exposure maps can be used to identify areas with low green exposure, i.e. possible locations where tree planting will have the greatest effect in terms of increasing green visual exposure. Strategic tree planting is especially important in the light of ongoing densification, where space for establishing large green areas is often limited and where planting single trees can represent an efficient way of increasing the overall green views. Fourth, by manipulating the input data, the method is applicable in scenario modelling and impact assessment. Manipulating the input tree canopy map (adding or removing trees) enables planners to compare different tree planting or felling scenarios and select those which result in the largest increase or smallest decrease in green visual exposure, respectively. Manipulating the input DSM on the other hand facilitates assessing the effect of planned construction projects on green visual exposure in the surroundings. Finally, thanks to the method's flexibility, application in areas beyond the scope of urban planning is also possible, for instance in landscape aesthetic and architectural studies (e.g. modelling exposure to landmarks or buildings) (Dramstad et al., 2006) or in visual impact assessment (e.g. modelling the visual impact of quarries or power plants).

The method developed in this paper further has the potential to further advance our knowledge on the relationship between green visual exposure and obtained benefits by providing reliable estimates of the amount of green visual exposure from human perspective. The continuous representation of the result can be combined e.g. with information on people's daily movements in exposure studies to gain a more in-depth and detailed insight into green exposure of individual participants. In environmental psychology studies, the method can easily be adjusted to reflect e.g., studied exposure range or dose–response curves. Further, the method complements research on olfactory and auditive sensory mapping (McLean, 2019).

5. Conclusion

The method developed in this paper underpins findings of earlier studies showing that geospatial modelling with viewshed analysis can be a reliable and highly accurate means of quantifying visual exposure to urban greenery from human perspective. For the specific case of urban trees, the method achieves increased accuracy compared to previous studies. Systematic assessment of the method's settings based on validation data shows that it is essential for the accuracy of the results to parametrise the viewshed analysis according to the variable visual significance of observed greenery. It also identifies reasonable default settings and illustrates how those influence the trade-off between accuracy and processing time, providing important insight for application purposes where a minor accuracy loss might be acceptable in return for shorter processing time. Furthermore, the implementation of the method significantly improves its computational performance to a degree that makes it usable at city-wide scale with high-resolution data on commodity hardware. The tool developed in this study represents a major technical step forward as it makes the method available as a practical and flexible tool for a broad range of research and practical applications. While developing the method and the tool, an R-package with a similar functionality has been made available, which further underpins the relevance of the method (Brinkmann & Labib, 2021). Therewith, the method contributes to the emerging number of quantitative methods that enable easier modelling of cultural ecosystem services that otherwise often are challenging to include in ecosystem accounting or landscape management.

Acknowledgements

We would like to thank Meta Berghauser Pont (Chalmers University of Technology, Sweden), Yngve Karl Frøyen (Norwegian University of Science and Technology) and David N. Barton (Norwegian Institute for Nature Research), as well as three anonymous reviewers, for their valuable feedback on the research. Our appreciation also goes to Alexandre Nollet (AgroParisTech), who contributed to collecting the validation data for this work. The work was supported by the Norwegian Research Council [grant number 160022/F40].

Appendix A. Supplementary data

Supplementary data to this article can be found online at https://doi.org/10.1016/j.landurbplan.2022.104395.

References

Aoki, Y., Yasuoka, Y., & Naito, M. (1985). Assessing the impression of street-side greenery. *Landscape Research, 10*, 9–13. https://doi.org/10.1080/01426398508706131

Bishop, I. D. (2003). Assessment of visual qualities, impacts, and behaviours, in the landscape, by using measures of visibility. *Environment and Planning B: Planning and Design, 30*, 677–688. https://doi.org/10.1068/b12956

Bishop, I. D., Lange, E., & Mahbubul, A. M. (2004). Estimation of the influence of view components on high-rise apartment pricing using a public survey and GIS modeling. *Environment and Planning B: Planning and Design, 31*, 439–452. https://doi.org/10.1068/b3042

Bolund, P., & Hunhammar, S. (1999). Ecosystem services in urban areas. *Ecological Economics, 29*, 293–301. https://doi.org/10.1016/S0921-8009(99)00013-0

Brabyn, L. (2015). Modelling landscape experience using "experions". *Applied Geography, 62*, 210–216. https://doi.org/10.1016/j.apgeog.2015.04.021

Brinkmann, S., & Labib, S.. GVI: R package for computing VGVI for Spatial Raster. https://doi.org/10.5281/zenodo.5060325.

Chamberlain, B. C., & Meitner, M. J. (2013). A route-based visibility analysis for landscape management. *Landscape and Urban Planning, 111*, 13–24. https://doi.org/10.1016/j.landurbplan.2012.12.004

De Vries, S., van Dillen, S. M. E., Groenewegen, P. P., & Spreeuwenberg, P. (2013). Streetscape greenery and health: Stress, social cohesion and physical activity as mediators. *Social Science and Medicine, 94*, 26–33. https://doi.org/10.1016/j.socscimed.2013.06.030

Demuzere, M., Orru, K., Heidrich, O., Olazabal, E., Geneletti, D., Orru, H., … Faehnle, M. (2014). Mitigating and adapting to climate change: Multi-functional and multi-scale assessment of green urban infrastructure. *Journal of Environmental Management, 146*, 107–115. https://doi.org/10.1016/j.jenvman.2014.07.025

Domingo-Santos, J.M., De-Villarán, R.F.-, 2017. Visibility Analysis, in: International Encyclopedia of Geography: People, the Earth, Environment and Technology. John Wiley & Sons, Ltd, Oxford, UK, pp. 1–14. 10.1002/9781118786352.wbieg0906.

Domingo-Santos, J. M., de Villarán, R. F., Rapp-Arrarás, Í., & de Provens, E.-C.-P. (2011). The visual exposure in forest and rural landscapes: An algorithm and a GIS tool. *Landscape and Urban Planning, 101*, 52–58. https://doi.org/10.1016/j.landurbplan.2010.11.018

Dramstad, W. E., Tveit, M. S., Fjellstad, W. J., & Fry, G. L. A. (2006). Relationships between visual landscape preferences and map-based indicators of landscape structure. *Landscape and Urban Planning, 78*, 465–474. https://doi.org/10.1016/j.landurbplan.2005.12.006

Ervin, S., & Steinitz, C. (2003). Landscape Visibility Computation: Necessary, but Not Sufficient. *Environment and Planning B: Planning and Design, 30*, 757–766. https://doi.org/10.1068/b2968

Falfán, I., Muñoz-Robles, C. A., Bonilla-Moheno, M., & MacGregor-Fors, I. (2018). Can you really see 'green'? Assessing physical and self-reported measurements of urban greenery. *Urban Forestry & Urban Greening, 36*, 13–21. https://doi.org/10.1016/j.ufug.2018.08.016

Fisher, P. (1994). Probable and fuzzy models of the viewshed operation. In M. F. Worboys (Ed.), *Innovations in GIS* (pp. 161–176). London, UK: Taylor & Francis.

Gomez-Baggethun, E., & Barton, D. N. (2013). Classifying and valuing ecosystem services for urban planning. *Ecological Economics, 86*, 235–245. https://doi.org/10.1016/j.ecolecon.2012.08.019

Grêt-Regamey, A., Bishop, I. D., & Bebi, P. (2007). Predicting the scenic beauty value of mapped landscape changes in a mountainous region through the use of GIS. *Environment and Planning B: Planning and Design, 34*, 50–67. https://doi.org/10.1068/b32051

Groß, M. (1991). The analysis of visibility-Environmental interactions between computer graphics, physics, and physiology. *Computers and Graphics, 15*, 407–415. https://doi.org/10.1016/0097-8493(91)90011-6

Hanssen, F., Barton, D. N., Venter, Z. S., Nowell, M. S., & Cimburova, Z. (2021). Utilizing LiDAR data to map tree canopy for urban ecosystem extent and condition accounts in Oslo. *Ecological Indicators, 130*, Article 108007. https://doi.org/10.1016/j.ecolind.2021.108007

Hazer, M., Formica, M. K., Dieterlen, S., & Morley, C. P. (2018). The relationship between self-reported exposure to greenspace and human stress in Baltimore, MD. *Landscape and Urban Planning, 169*, 47–56. https://doi.org/10.1016/j.landurbplan.2017.08.006

Helbich, M. (2018). Toward dynamic urban environmental exposure assessments in mental health research. *Environmental Research, 161*, 129–135. https://doi.org/10.1016/j.envres.2017.11.006

Helbich, M., Yao, Y., Liu, Y., Zhang, J., Liu, P., & Wang, R. (2019). Using deep learning to examine street view green and blue spaces and their associations with geriatric depression in Beijing, China. *Environment International, 126*, 107–117. https://doi.org/10.1016/j.envint.2019.02.013

Iverson, W. D. (1985). And That's about the size of it: Visual magnitude as a measurement of the physical landscape. *Landscape Journal, 4*, 14–22.

Kaplan, R. (2001). The nature of the view from home. *Environment and Behavior, 33*, 507–542.

Keniger, L., Gaston, K., Irvine, K., & Fuller, R. (2013). What are the Benefits of Interacting with Nature? *International Journal of Environmental Research and Public Health, 10*, 913–935. https://doi.org/10.3390/ijerph10030913

Ki, D., & Lee, S. (2021). Analyzing the effects of Green View Index of neighborhood streets on walking time using Google Street View and deep learning. *Landscape and Urban Planning, 205*, Article 103920. https://doi.org/10.1016/j.landurbplan.2020.103920

Labib, S. M., Huck, J. J., & Lindley, S. (2021). Modelling and mapping eye-level greenness visibility exposure using multi-source data at high spatial resolutions. *Science of the Total Environment, 755*, Article 143050. https://doi.org/10.1016/j.scitotenv.2020.143050

Larkin, A., & Hystad, P. (2019). Evaluating street view exposure measures of visible green space for health research. *Journal of Exposure Science & Environmental Epidemiology, 29*, 447–456. https://doi.org/10.1038/s41370-018-0017-1

Łaszkiewicz, E., & Sikorska, D. (2020). Children's green walk to school: An evaluation of welfare-related disparities in the visibility of greenery among children. *Environmental Science & Policy, 110*, 1–13. https://doi.org/10.1016/j.envsci.2020.05.009

Llobera, M. (2003). Extending GIS-based visual analysis: The concept of visualscapes. *International Journal of Geographical Information Science, 17*, 25–48. https://doi.org/10.1080/713811741

Lottrup, L., Stigsdotter, U. K., Meilby, H., & Claudi, A. G. (2015). The workplace window view: A determinant of office workers' work ability and job satisfaction. *Landscape Research, 40*, 57–75. https://doi.org/10.1080/01426397.2013.829806

McLean, K. (2019). Sensory maps. In A. Kobayashi (Ed.), *International Encyclopaedia of Human Geography* (2nd edition, pp. 153–168). Elsevier.

Millennium Ecosystem Assessment. (2003). *Ecosystems and human well-being: A framework for assessment*. Washington, DC: Island Press.

Minelli, A., Marchesini, I., Taylor, F. E., De Rosa, P., Casagrande, L., & Cenci, M. (2014). An open source GIS tool to quantify the visual impact of wind turbines and photovoltaic panels. *Environmental Impact Assessment Review, 49*, 70–78. https://doi.org/10.1016/j.eiar.2014.07.002

Mouratidis, K. (2019). The impact of urban tree cover on perceived safety. *Urban Forestry & Urban Greening, 44*, Article 126434. https://doi.org/10.1016/j.ufug.2019.126434

Murgoitio, J. J., Shrestha, R., Glenn, N. F., & Spaete, L. P. (2013). Improved visibility calculations with tree trunk obstruction modeling from aerial LiDAR. *International Journal of Geographical Information Science, 27*, 1865–1883. https://doi.org/10.1080/13658816.2013.767460

Neteler, M., Bowman, M. H., Landa, M., & Metz, M. (2012). GRASS GIS: A multi-purpose open source GIS. *Environmental Modelling and Software, 31*, 124–130. https://doi.org/10.1016/j.envsoft.2011.11.014

Nowak, D. J. (2017). Assessing the benefits and economic values of trees. In F. Ferrini, C. C. K. van den Bosch, & A. Fini (Eds.), *Handbook of Urban Forestry* (pp. 152–163). NY: Routledge.

Nutsford, D., Pearson, A. L., Kingham, S., & Reitsma, F. (2016). Residential exposure to visible blue space (but not green space) associated with lower psychological distress in a capital city. *Health & Place, 39*, 70–78. https://doi.org/10.1016/j.healthplace.2016.03.002

Nutsford, D., Reitsma, F., Pearson, A. L., & Kingham, S. (2015). Personalising the viewshed: Visibility analysis from the human perspective. *Applied Geography, 62*, 1–7. https://doi.org/10.1016/j.apgeog.2015.04.004

Office for National Statistics (ONS). (2019). UK natural capital: Urban accounts [WWW Document] accessed 1.6.21 https://www.ons.gov.uk/economy/environmentalaccounts/bulletins/uknaturalcapital/urbanaccounts.

Ogburn, D. E. (2006). Assessing the level of visibility of cultural objects in past landscapes. *Journal of Archaeological Science, 33*, 405–413. https://doi.org/10.1016/j.jas.2005.08.005

Petrasova, A., Harmon, B., Petras, V., Mitasova, H., 2015. Viewshed Analysis, in: Tangible Modeling with Open Source GIS. Springer International Publishing, Cham, pp. 77–82. 10.1007/978-3-319-25775-4_6.

Qiang, Y., Shen, S., & Chen, Q. (2019). Visibility analysis of oceanic blue space using digital elevation models. *Landscape and Urban Planning, 181*, 92–102. https://doi.org/10.1016/j.landurbplan.2018.09.019

Reid, C., Clougherty, J., Shmool, J., & Kubzansky, L. (2017). Is all urban green space the same? A comparison of the health benefits of trees and grass in New York City. *International Journal of Environmental Research and Public Health, 14*, 1411. https://doi.org/10.3390/ijerph14111411

Rzotkiewicz, A., Pearson, A. L., Dougherty, B. V., Shortridge, A., & Wilson, N. (2018). Systematic review of the use of Google Street View in health research: Major themes, strengths, weaknesses and possibilities for future research. *Health and Place, 52*, 240–246. https://doi.org/10.1016/j.healthplace.2018.07.001

Schroeder, H., & Cannon, W. N. (1983). The esthetic contribution of trees to residential streets in Ohio towns. *Journal of Arboriculture, 9*, 237–243.

Sun, Y., Wang, X., Zhu, J., Chen, L., Jia, Y., Lawrence, J. M., … Wu, J. (2021). Using machine learning to examine street green space types at a high spatial resolution: Application in Los Angeles County on socioeconomic disparities in exposure. *Science of The Total Environment, 147653*. https://doi.org/10.1016/j.scitotenv.2021.147653

Tabrizian, P., Baran, P. K., Van Berkel, D., Mitasova, H., & Meentemeyer, R. (2020). Modeling restorative potential of urban environments by coupling viewscape analysis of lidar data with experiments in immersive virtual environments. *Landscape and Urban Planning, 195*, Article 103704. https://doi.org/10.1016/j.landurbplan.2019.103704

TEEB, 2010. The Economics of Ecosystems and Biodiversity Ecological and Economic Foundations. Edited by Pushpam Kumar. Earthscan, London and Washington. Routledge. doi: 10.1080/19390459.2013.763324.

Thayer, R. L., & Atwood, B. G. (1978). Plants, complexity, and pleasure in urban and suburban environments. *Environmental Psychology and Nonverbal Behavior, 3*, 67–76. https://doi.org/10.1007/BF01135604

Toma, L., Zhuang, Y., Richard, W., Metz, M., 2020. GRASS GIS: r.viewshed module.

Travis, M.R., Elsner, G.H., Iverson, W.D., Johnson, C.G., 1975. VIEWIT: computation of seen areas, slope, and aspect for land-use planning. General Technical Report PSW-11/1975.

Troy, A., Morgan Grove, J., & O'Neil-Dunne, J. (2012). The relationship between tree canopy and crime rates across an urban-rural gradient in the greater Baltimore region. *Landscape and Urban Planning, 106*, 262–270. https://doi.org/10.1016/j.landurbplan.2012.03.010

Tyrväinen, L., & Miettinen, A. (2000). Property prices and urban forest amenities. *Journal of Environmental Economics and Management, 39*, 205–223. https://doi.org/10.1006/jeem.1999.1097

Ulrich, R. (1984). View through a window may influence recovery from surgery. *Science, 224*, 420–421. https://doi.org/10.1126/science.6143402

Venter, Z.S., Sydenham, M.A.K., 2021. Operational land cover mapping at continental scale and 10 m resolution over Europe (ELC10). ISPRS Journal of Photogrammetry and Remote Sensing submitted.

Villeneuve, P. J., Ysseldyk, R. L., Root, A., Ambrose, S., DiMuzio, J., Kumar, N., … Rainham, D. (2018). Comparing the normalized difference vegetation index with the google street view measure of vegetation to assess associations between greenness, walkability, recreational physical activity, and health in Ottawa, Canada. *International Journal of Environmental Research and Public Health, 15*, 1719. https://doi.org/10.3390/ijerph15081719

Wang, R., Helbich, M., Yao, Y., Zhang, J., Liu, P., Yuan, Y., & Liu, Y. (2019). Urban greenery and mental wellbeing in adults: Cross-sectional mediation analyses on multiple pathways across different greenery measures. *Environmental Research, 176*, Article 108535. https://doi.org/10.1016/j.envres.2019.108535

Wang, W., Lin, Z., Zhang, L., Yu, T., Ciren, P., & Zhu, Y. (2019). Building visual green index: A measure of visual green spaces for urban building. *Urban Forestry & Urban Greening, 40*, 335–343. https://doi.org/10.1016/j.ufug.2018.04.004

Ward Thompson, C., Aspinall, P., Roe, J., Robertson, L., & Miller, D. (2016). Mitigating stress and supporting health in deprived urban communities: The importance of green space and the social environment. *International Journal of Environmental Research and Public Health, 13*, 440. https://doi.org/10.3390/ijerph13040440

Wheatley, D. (1995). Cumulative Viewshed Analysis: A GIS-based method for investigating intervisibility, and its archaeological application. In Z. Stancic, & G. Lock (Eds.), *Archaeology and Geographic Information Systems: A European Perspective* (pp. 171–185). London: Routlege.

Wolfe, M. K., & Mennis, J. (2012). Does vegetation encourage or suppress urban crime? Evidence from Philadelphia, PA. *Landscape and Urban Planning, 108*, 112–122. https://doi.org/10.1016/j.landurbplan.2012.08.006

Yan, J., Zhou, W., Han, L., & Qian, Y. (2018). Mapping vegetation functional types in urban areas with WorldView-2 imagery: Integrating object-based classification with phenology. *Urban Forestry & Urban Greening, 31*, 230–240. https://doi.org/10.1016/j.ufug.2018.01.021

Yang, J., Zhao, L., McBride, J., & Gong, P. (2009). Can you see green? Assessing the visibility of urban forests in cities. *Landscape and Urban Planning, 91*, 97–104. https://doi.org/10.1016/j.landurbplan.2008.12.004

Zelnik-Manor, L., Peters, G., Perona, P., 2005. Squaring the circle in panoramas, in: Tenth IEEE International Conference on Computer Vision (ICCV'05) Volume 1. IEEE, pp. 1292-1299 Vol. 2. 10.1109/ICCV.2005.231.

Norwegian mapping authority Høydedata Oslo kommune laserskanning 2019 (version 2019). (). Retrieved from https://kartkatalog.geonorge.no/metadata/hoeydedata-oslo-kommune-laserskanning-2019/dfcf22c8-6484-4c9f-9cce-c1c9985f0461 .